Letter

Evidence of random spin-singlet state in the three-dimensional quantum spin liquid candidate $Sr_3CuNb_2O_9$

S. M. Hossain,[1] S. S. Rahaman,[2] H. Gujrati,[1] Dilip Bhoi,[3] A. Matsuo,[3] K. Kindo,[3] M. Kumar,[2,*] and M. Majumder[1,†]

[1]*Department of Physics, Shiv Nadar Institution of Eminence, Gautam Buddha Nagar, Uttar Pradesh 201314, India*

[2]*S.N. Bose National Centre for Basic Sciences, Salt Lake, Kolkata 700106, India*

[3]*The Institute for Solid State Physics, University of Tokyo, Kashiwa, Chiba 277-8581, Japan*

(Received 2 February 2024; revised 11 May 2024; accepted 27 June 2024; published 18 July 2024)

Disorder is ubiquitous in any quantum many-body system and is usually considered to be an obstacle to the elucidation of the underlying physics of complex systems, but its presence can often introduce exotic phases of matter that cannot generally be realized in a clean system. We report here a detailed experimental and theoretical study of the magnetic properties of the highly disordered material $Sr_3CuNb_2O_9$, which exhibits random site mixing between Cu and Nb. The magnetic moments (Cu^{2+}) are arranged in a quasicubic (three-dimensional) manner, leading to a high degree of frustration with a Curie-Weiss temperature θ_{CW} of about -60 K without any long-range magnetic ordering down to 466 mK. These observations suggest that $Sr_3CuNb_2O_9$ is a candidate for a quantum spin liquid (QSL). More interestingly, the susceptibility ($\chi = M/\mu_0 H$) and C_m/T (C_m is the magnetic part of the heat capacity) follow a power-law behavior with decreasing temperature. In addition, $M(T, \mu_0 H)$ and $C_m(T, \mu_0 H)/T$ show scaling relationships over a wide range of temperatures and fields. This unusual behavior with respect to the conventional behavior of a QSL can be discussed qualitatively as the coexistence of a disorder-induced random spin-singlet (RSS) state and a QSL state. A quantitative description is given by numerical calculations considering a power-law probability distribution $P(J) \propto J^{-\gamma}$ (J is the exchange interaction) of random spin singlets. The parameters extracted from the numerical calculations are in excellent agreement with the experimental data. Furthermore, the analytical results are also consistent with the power-law and scaling behavior of χ and $C_m(T, \mu_0 H)/T$ as a whole. Thus, our comprehensive experimental and theoretical analysis provides evidence of the stabilization of the RSS state in a three-dimensional lattice.

DOI: 10.1103/PhysRevB.110.L020406

Introduction. The presence of disorder is inevitable in any real-life quantum many-body system, and it hinders us from elucidating the actual physics of a system. More specifically, the effects of disorder on the phases or phase transitions in quantum many-body systems are reflected by the disappearance of spontaneous symmetry breaking or the smearing out of the singularities associated with phase transitions and critical phases [1]. On the contrary, there are also examples of exotic ground states and new phenomena driven by disorder which cannot be realized in a clean or disorder-free system. Thus, discovering and characterizing those ground states in a quantum many-body system where the interplay of disorder and quantum fluctuations exists are a current field of study in condensed matter physics [1,2]. These systems are also crucial for several application purposes; e.g., they can be the key elements for memories and state transfer channels in quantum computing [3–6]. One of the first prominent examples of disorder-driven states is Anderson localization, where the wave function of noninteracting quantum particles is highly localized near a point in space due to a strong random potential [7,8]. Recently, disorder-driven topological Anderson localization was also observed [9,10]. Quasiparticle interference is a powerful experimental tool, and it originates because of the presence of disorder and helps us to explore the momentum space information in a two-dimensional (2D) system [11]. Disorder-driven phenomena are also often observed in correlated many-body systems, e.g., the Kondo disorder state and quantum Griffiths phase, which shows exotic non-Fermi-liquid behaviors [1,12–14]. Experimentally and theoretically, it was also observed that the presence of strong disorder can turn the first-order magnetic phase transition into a second-order phase transition near the quantum critical point, and thus, a disorder-induced quantum critical point can be obtained [2,15].

The effects of disorder in frustrated magnets is currently a focus area. Frustration may lead to huge accidental degeneracy of different spin configurations, and the ground state is the superposition of the degenerate states, known as the quantum spin liquid (QSL) state. In the QSL state, due to the absence of spontaneous symmetry breaking, the spins are dynamic even at $T = 0$ K, and one can expect exotic fractionalized excitations [16–18]. The presence of disorder in a frustrated system gives rise to a glassy state, the spin glass state [19]. The superlattice structure produced by site disorder may also give rise to a frustrated triangular lattice and, further, may lead to the observation of a QSL state [20]. Very recently, Kimchi *et al.* pointed out that in some disordered frustrated

*Contact author: manoranjan.kumar@bose.res.in

†Contact author: mayukh.majumder@snu.edu.in

systems, peculiar features of the heat capacity and magnetization can be qualitatively explained as the presence of a "random spin-singlet" (RSS) state admixed with a QSL state [21]. The RSS state was first discussed for doped semiconductors in which the antiferromagnetic exchange energies follow a power-law probability distribution due to the presence of disorder [22–24]. Further, this idea of a RSS state was also extended to two and three dimensions [25–28] for doped semiconductors. However, only a handful of the 2D frustrated systems show such exotic states where the RSS state and QSL coexist [29–32], and so far, the presence of such a state has not been observed in any three-dimensional (3D) frustrated system experimentally. Note that in some 3D pyrochlore systems, the signature of a QSL-like state was interpreted to be due to a RSS state, but the probability distribution of exchange energies was not a power-law probability distribution [33]. Thus, discovering new three-dimensional systems with strong frustration along with disorder and elucidating the complex ground state qualitatively and quantitatively is a primary goal in this field. Needless to say, stabilizing such a state in a 3D lattice is inherently more challenging than in low-dimensional systems, primarily because the enhanced dimensionality reduces quantum fluctuations and hence there is a greater tendency to order magnetically.

In this Letter, we report a detailed study of the three-dimensional quasicubic system $Sr_3CuNb_2O_9$. Magnetization and heat capacity measurements down to 466 mK indicate the absence of long-range magnetic ordering (LRO) despite strong exchange interactions (of the order of -60 K) between Cu^{2+} moments and thus establish $Sr_3CuNb_2O_9$ as a 3D QSL candidate. Furthermore, the power-law divergence of susceptibility and heat capacity, along with the scaling behaviors of magnetization and heat capacity, indicate the presence of a RSS state admixed with a QSL due to the presence of strong Cu/Nb site disorder. Furthermore, numerical and analytical calculations describe the experimental data quantitatively.

Crystal structure. $Sr_3CuNb_2O_9$ was synthesized via a conventional solid-state reaction technique (details are discussed in the Supplemental Material [34]; see also Ref. [35] therein). $Sr_3CuNb_2O_9$ belongs to a family of triple-perovskite crystal structures with the general formula $A_3B_3O_9$, as shown in Fig. 1(a). The compound stabilizes in a tetragonal crystal structure of space group $P4/mmm$ (space group number 123), with lattice parameters $a = b \approx 3.953$ Å, $c = 4.089$ Å, and $\alpha = \beta = \gamma = 90^\circ$ obtained from powder x-ray diffraction (PXRD) Rietveld refinement [Fig. 1(c)]. No extra peaks represent the existence of single-phase formation. Most importantly, no superlattice peaks have been detected, indicating a random distribution of Cu and Nb atoms, in contrast to $Sr_3CuSb_2O_9$ [20]. Thus, the magnetic skeleton is formed by Cu atoms randomly distributed over Nb sites, with occupancy ratios of 1/3 and 2/3, respectively, and the in-plane distance between magnetic ions is ≈ 3.95 Å, whereas the out-of-plane distance is ≈ 4.07 Å, making it an almost cubic magnetic lattice structure, as shown in Fig. 1(b). Such a quasicubic 3D structure, if one considers the next-nearest-neighbor interactions along with nearest-neighbor ones, may give rise to a 3D frustrated lattice. Thus, the present compound, on the one hand, may provide a 3D frustrated lattice and, on the other hand, provides strong disorder (random site disorder of Cu and Nb), which may then be favorable for realizing a RSS state. In order to verify our expectation from the structural analysis, we explore the ground state by performing detailed magnetization and heat capacity measurements in a broad temperature-field region.

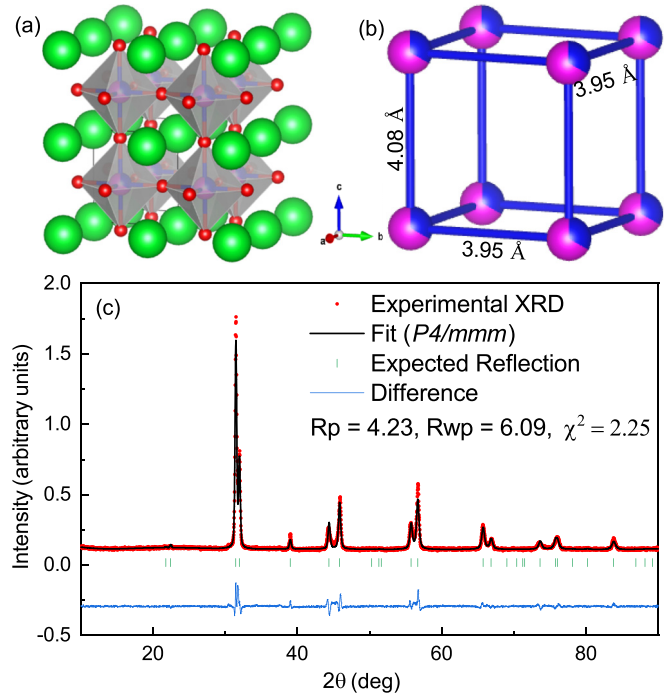

FIG. 1. (a) Magnetic sites forming an octahedral environment with the oxygen atoms (red) and the green spheres, showing strontium atoms intercalated in between. (b) Arrangement of the magnetic Cu^{2+} (blue) sharing the same site with the nonmagnetic Nb^{5+} (magenta). (c) A clean XRD pattern shows the absence of any impurity and was analyzed with the Rietveld refinement method.

Magnetization. Magnetic susceptibility ($\chi = M/\mu_0 H$) was measured as a function of temperature at different applied magnetic fields. No anomaly associated with LRO was observed down to 1.85 K, as seen from Fig. 2(a). The susceptibility data between 100 and 300 K, measured at an applied magnetic field of 1 T, were fitted with the Curie-Weiss law ($\chi = \frac{C}{T-\theta_{CW}} + \chi_0$), shown as a solid line in Fig. 2(a). The Curie-Weiss temperature θ_{CW} obtained is ≈ -60 K, with a Curie constant $C = 0.49$ cm^3 K mol^{-1}. The negative sign indicates the nature of exchanges is antiferromagnetic with a high degree of frustration, defined as $f = \theta_{CW}/T_N$. For any magnetic system, θ_{CW} indicates the strength of exchange interactions between magnetic moments, and T_N is the ordering temperature. In the present systems, even though the moments are highly correlated with high θ_{CW}, the system cannot go to an LRO state at least down to 1.85 K due to strong frustration. The effective moment was calculated using the formula $\mu_{eff} = \sqrt{8C}$ gives $1.98\mu_B$, where C is the Curie constant obtained from the $1/\chi$ vs T fitting shown in Fig. 2(a). This indicates that the magnetic ions are in the Cu^{2+} ($S = 1/2$) state. Furthermore, the absence of branching in χ between the zero-field cooling and field cooling measured at 50 Oe rules out the possibility of a spin freezing state (e.g., a spin glass), at least down to 1.85 K [Fig. 2(b)]. Thus, magnetization

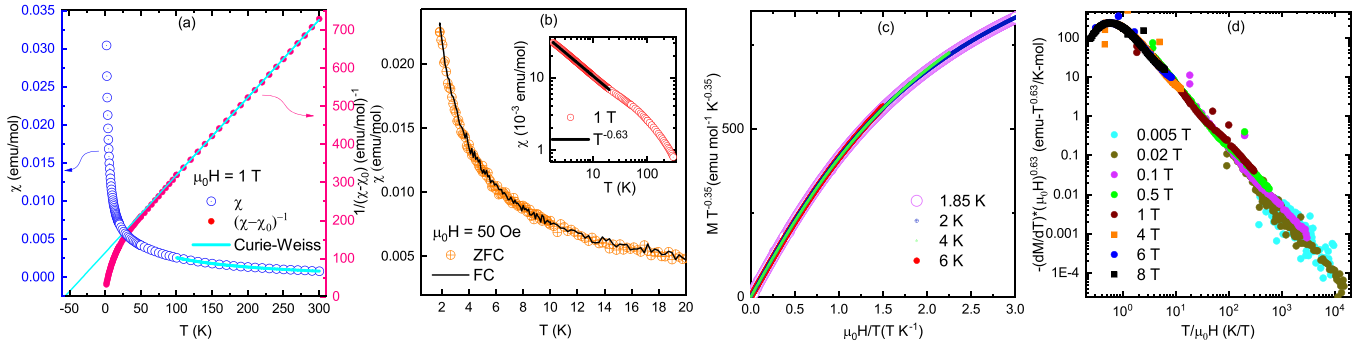

FIG. 2. (a) χ versus temperature at an applied magnetic field of 1 T (ZFC) and extrapolation of the Curie-Wiess fit (ranging from 100 to 300 K) in the inverse susceptibility data. (b) ZFC and FC data at 50 Oe applied magnetic field; the inset shows the power-law behavior with the exponent $\gamma = 0.63$. (c) Scaling behavior of the magnetization data with respect to field at different temperatures with an exponent of $\gamma - 1 = 0.35$. (d) Scaling of the magnetization with respect to the temperature, showing excellent data collapse in a wide applied magnetic field range from 50 Oe to 8 T.

measurements ensure that $Sr_3CuNb_2O_9$ can be considered a highly frustrated magnetic system promising to have a QSL ground state.

More interestingly, if one closely observes the temperature dependence of χ, then one can see that χ follows a power-law behavior ($T^{-\gamma}$) between 20 and 1.85 K, with γ being 0.63. Such a power-law behavior was predicted to be a signature of a RSS state in a frustrated system [21]. Along with the power law in χ, the M versus $\mu_0 H$ data at different temperatures also collapse in one curve following a scaling behavior, as shown in Fig. 2(c) as $MT^{\gamma-1}$ against $\mu_0 H/T$. A scaling has even been observed in $(dM/dT) \times (\mu_0 H)^{\gamma}$ versus $T/\mu_0 H$. All these power-law and scaling behaviors support the presence of the predicted RSS state admixed with a QSL state.

Heat capacity. Heat capacity $C_p(T, \mu_0 H)$ measurements were performed from 300 K down to 466 mK at various applied magnetic fields to explore the ground state of $Sr_3CuNb_2O_9$. Figure 3(a) shows C_p versus T at different applied magnetic fields. The absence of any λ-like anomaly indicates that $Sr_3CuNb_2O_9$ avoids any LRO down to 466 mK even though there is a strong correlation between magnetic moments, thus establishing that $Sr_3CuNb_2O_9$ is a 3D QSL candidate with a high degree of frustration ($f = \theta_{CW}/T_{min} \simeq 120$, where T_{min} represents the lowest temperature for which heat capacity has been measured). In general, C_p/T follows either exponential behavior or a power law (T^{γ}) for gapped and gapless QSLs, respectively [36,37]. In contrast to this expectation, C_p/T follows the power-law behavior of $T^{-\gamma}$ in the present system at zero applied magnetic field. To get a qualitative description of the C_p data, we modeled it by considering three contributions:

$$C_p(T, \mu_0 H) = C_{ph} + C_{Sch} + C_{power\text{-}law}, \tag{1}$$

where $C_{power\text{-}law} = A_{power\text{-}law} T^{1-\gamma}$ [29]. The other two terms, C_{ph} and C_{Sch}, represent the phonon contribution and two-level Schottky contribution (representing the hump), respectively. At sufficiently low temperatures, the phonon contribution behaves as $C_{ph} = \beta_{ph} T^3$, where β_{ph} is the Debye coefficient, and

$$C_{Sch} = A_{Sch} R \left[\frac{\Delta(\mu_0 H)}{k_B T}\right]^2 \frac{e^{\left(\frac{\Delta(\mu_0 H)}{k_B T}\right)}}{[1 + e^{\left(\frac{\Delta(\mu_0 H)}{k_B T}\right)}]^2}, \tag{2}$$

where $\frac{\Delta}{k_B}$ represents the energy gap.

$C_m(\mu_0 H = 0)/T$ at zero field is plotted as a function of temperature in Fig. 3(b), estimated by subtracting the phonon (C_{ph}) and Schottky contributions (because of the 1.8% weakly coupled impurities; for details see the Supplemental Material [34] and Refs. [20,30,38–42] therein) from the total

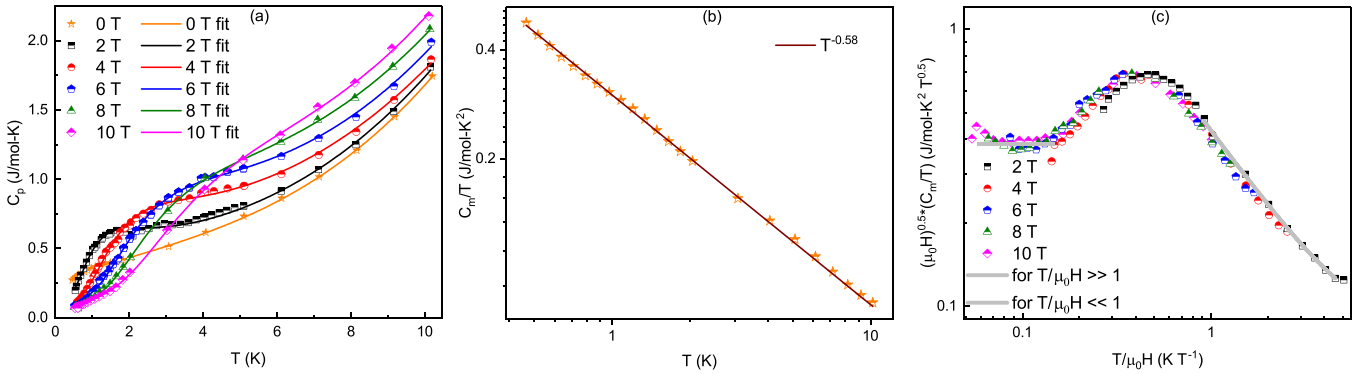

FIG. 3. (a) Temperature dependence of $C(T, \mu_0 H)$ at different applied magnetic fields. Solid lines show the fit considering three different contributions described in the text. (b) Power-law fit of C_m/T (at 0 T) as a function of temperature with an exponent of 0.58. (c) Scaling of $C_m(T, \mu_0 H)/T$.

C_p. $C_m(\mu_0 H = 0)/T$ shows a power-law divergence with an exponent $\gamma = 0.58$ with decreasing temperature. Also, note that the exponent γ is in agreement with the obtained γ from magnetization measurements.

From the qualitative analysis of C_p it is now clear that the spins are correlated (as seen from high $\theta_{\rm CW}$) and may form random singlets by a power-law distribution of exchange interactions due to the presence of strong site disorder. Because of the power-law distribution of the exchange interactions (responsible for forming singlets), the excitations are gapless overall, giving rise to the power-law behavior in the magnetization or heat capacity and, eventually, the scaling behaviors. These correlated spins (which form the singlets) may also form a resonating state due to the presence of strong frustration, which may give rise to a QSL behavior.

Kimchi *et al.* [21] pointed out that the magnetic contribution of the total heat capacity at finite fields [represented by $C_m(\mu_0 H) = C_p - C_{\rm ph}$; see the Supplemental Material [34] for details and also see Ref. [29] therein] for this disorder-induced state collapses into a single curve of the form

$$\frac{C_m[\mu_0 H, T]}{T} \sim \frac{1}{(\mu_0 H)^{\gamma}} F_q\left[\frac{T}{\mu_0 H}\right], \tag{3}$$

where $Fq(X)$ is a scaling function which is determined by the energy distribution of the singlets,

$$F_q[X] \sim \begin{cases} X^q & X \ll 1, \\ X^{-\gamma}\left(1 + \frac{c_0}{X^2}\right) & X \gg 1, \end{cases} \tag{4}$$

where $q = 1$ and $q = 0$ represent the cases with and without Dzyaloshinskii-Moriya (DM) interactions in the effective low-energy theory coupling the orphan spins, respectively. Figure 3(b) represents $(\mu_0 H)^{0.5} \times C_m/T$ as a function of $T/\mu_0 H$ in which all the C_m data points fall on top of each other and thus validates the scaling relationship as proposed by the theory. In the range where $X \ll 1$, the data saturate, indicating the absence of DM interactions, whereas in the limit of $X \gg 1$, the data agree reasonably well with the predicted scaling function [Fig. 3(c)]. It should be pointed out that the scaling behavior still holds for the total heat capacity (see Fig. 6 of the Supplemental Material [34]), except for the high-temperature region where the lattice contribution dominates.

Thus, the detailed magnetization and heat capacity measurements in a broad range of temperatures and fields indicate the coexistence of a RSS state and a QSL state in three-dimensional $Sr_3CuNb_2O_9$. Even though the experimental data represented here qualitatively match the theoretical prediction, a more quantitative description will be crucial to elucidate the underlying complex physics.

Theory. We further carried out numerical calculations to get a quantitative description of the temperature and field dependence of magnetization and heat capacity to confirm the possibility of the presence of a RSS state in $Sr_3CuNb_2O_9$. To understand the magnetic properties of the material we first analyzed the percentage distribution of Cu in various clusters with a size of up to a $30 \times 30 \times 30$ cubic lattice for the compound $Sr_3CuNb_2O_9$ with only 33% Cu. The distance between the two Cu atoms sitting in the two nearest octahedra of the present compound is approximately 4 Å; therefore, a spin is part of the cluster if the distance of the spin is less than or equal to 4 Å from any other spin in the cluster, and with this criterion the percentage distribution of the Cu atoms decays exponentially with cluster size L, as shown in the Supplemental Material, which gives the details of the calculation [34]. The most dominating spin clusters are free spins, and some of these spins may form weakly interacting Cu structures with random exchange as the distances among the spins are larger than 4 Å and random. These spins can have comparable nearest and next-nearest exchanges due to their distribution in three-dimensional space. Therefore, these weakly interacting frustrated spins can be treated as random dimer singlets with a broad distribution of exchanges. Other spin clusters bigger than the dimer are very small in number and may have a negligible effect on the magnetic properties of the material. Hence, we adopt an isotropic dimer Heisenberg spin-1/2 model Hamiltonian, incorporating the distribution of exchanges. This idea is inspired by the spin-1/2 model proposed by Dasgupta and Ma [22] for highly disordered one-dimensional systems, as well as the model presented by Bhatt and Lee [25] for highly disordered two- and three-dimensional systems. The dimer model can be written as

$$H = \sum_i J_i S_{i,1} S_{i,2} = \sum_i H_i, \tag{5}$$

where H_i is the ith isolated dimer Hamiltonian for spins 1 and 2 and J_i is the isotropic exchange interaction of the ith

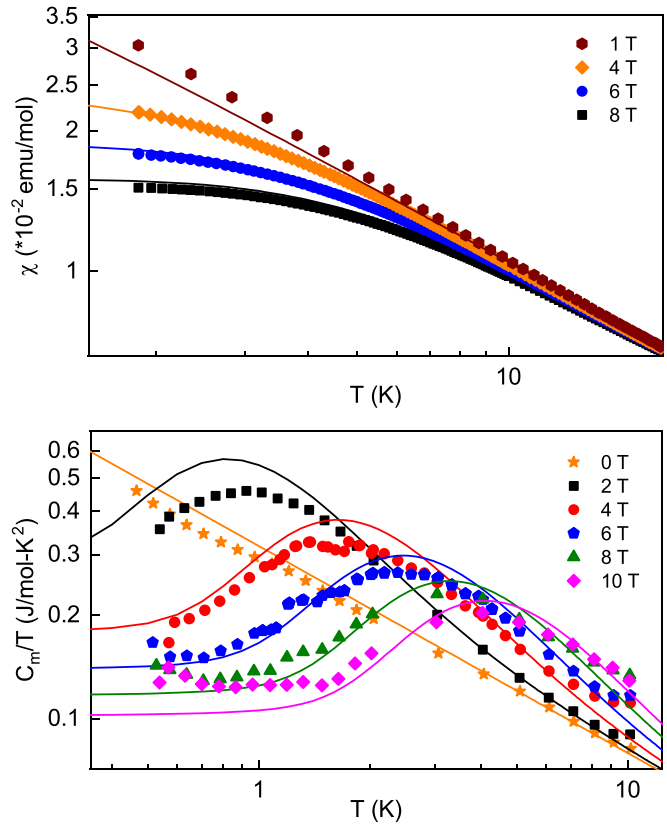

FIG. 4. Top: Temperature dependence of χ (obtained experimentally), represented by the scattered points; the solid lines indicate the data obtained numerically. Bottom: The solid lines and the scattered points represent experimentally and numerically obtained data of C_m/T.

dimer. We assume J_i can take any continuous value (between 0 and 1 in the reduced unit), and it follows the distribution $P(J) = J^{-\gamma}$; i.e., a smaller J has a higher probability distribution. A detailed description of the calculation is given in the Supplemental Material [34].

We use $g = 2.22$, the average $J = \langle J_i \rangle \approx 72$ K, and $\gamma = 0.6$ to fit the experimental curve of $C_m(T, \mu_0 H)/T$ and $\chi(T)$. $\frac{M}{H}$ for four different fields are shown in the top panel of Fig. 4, and the $\chi(=\frac{M}{H})$ curves show a power-law decay as a function of temperature. The experimental curve of $C_m(T, \mu_0 H)/T$ is shown as points, and the theoretical curve is shown as lines for six different magnetic fields; all the experimental curves can be fitted well with the theoretical curves, as shown in bottom panel of Fig. 4. In the bottom panel of Fig. 4, the linear behavior of the C_m/T plot clearly shows the power-law behavior for zero field, but the finite-field data show criticality as a function of T and H. This behavior is well known as data collapse in $\frac{T}{H}$ for the resonating limit $|J - H| < k_B T$. We notice that both $C_m(T, \mu_0 H)/T$ and χ can be fitted well with the experimental data with the same exponent, which is 0.6 in this case. We analyze these results for different limits of temperature and field in the Supplemental Material [34].

Thus, our numerical calculations quantitatively establish that the temperature and field dependence of the magnetization and heat capacity are due to the presence of a disorder-driven RSS state.

Conclusion. We studied a novel disorder-induced state in great detail. We reported a comprehensive experimental and theoretical investigation of the compound $Sr_3CuNb_2O_9$. The disorder introduced by site mixing between Cu and Nb and the frustration due to competing nearest neighbors and next-nearest neighbors of the three-dimensional quasicubic lattice gives rise to an exotic state in which the RSS state coexists with a QSL. Numerical calculations further gave a quantitative description of the experimental results and provided evidence of the realization of the RSS state in a three-dimensional lattice. Analytical calculations again confirmed the experimentally observed behaviors of χ and $C_m(T, \mu_0 H)/T$. These observations established $Sr_3CuNb_2O_9$ as one of the rare compounds in which such a RSS occurs in a 3D lattice.

Acknowledgments. S.M.H. and M.M. would like to acknowledge the UGC-DAE Collaborative Research Scheme (Ref. No. CRS/2021-22/01/393) for funding. M.K. thanks DST-SERB for funding through Project No. CRG/2020/000754.

[1] T. Vojta, Disorder in quantum many-body systems, Annu. Rev. Condens. Matter Phys. **10**, 233 (2019).
[2] A. G. Green, G. Conduit, and F. Krüger, Quantum order-by-disorder in strongly correlated metals, Annu. Rev. Condens. Matter Phys. **9**, 59 (2018).
[3] R. Nandkishore and D. A. Huse, Many-body localization and thermalization in quantum statistical mechanics, Annu. Rev. Condens. Matter Phys. **6**, 15 (2015).
[4] N. Y. Yao, L. Jiang, A. V. Gorshkov, Z.-X. Gong, A. Zhai, L.-M. Duan, and M. D. Lukin, Robust quantum state transfer in random unpolarized spin chains, Phys. Rev. Lett. **106**, 040505 (2011).
[5] J. Smith, A. Lee, P. Richerme, B. Neyenhuis, P. W. Hess, P. Hauke, M. Heyl, D. A. Huse, and C. Monroe, Many-body localization in a quantum simulator with programmable random disorder, Nat. Phys. **12**, 907 (2016).
[6] A. Kitaev, Anyons in an exactly solved model and beyond, Ann. Phys. (NY) **321**, 2 (2006).
[7] P. W. Anderson, Absence of diffusion in certain random lattices, Phys. Rev. **109**, 1492 (1958).
[8] A. Lagendijk, B. van Tiggelen, and D. S. Wiersma, Fifty years of Anderson localization, Phys. Today **62**(8), 24 (2009).
[9] Q. Lin, T. Li, L. Xiao, K. Wang, W. Yi, and P. Xue, Observation of non-Hermitian topological Anderson insulator in quantum dynamics, Nat. Commun. **13**, 3229 (2022).
[10] R. Bhatt and A. Krishna, Topology and many-body localization, Ann. Phys. (NY) **435**, 168438 (2021).
[11] N. Avraham, J. Reiner, A. Kumar-Nayak, N. Morali, R. Batabyal, B. Yan, and H. Beidenkopf, Quasiparticle interference studies of quantum materials, Adv. Mater. **30**, 1707628 (2018).
[12] S.-S. Lee, Recent developments in non-Fermi liquid theory, Annu. Rev. Condens. Matter Phys. **9**, 227 (2018).
[13] E. F. Shender and P. C. W. Holdsworth, Order by disorder and topology in frustrated magnetic systems, in *Fluctuations and Order: The New Synthesis*, edited by M. Millonas (Springer, New York, 1996), pp. 259–279.
[14] D. Bergman, J. Alicea, E. Gull, S. Trebst, and L. Balents, Order-by-disorder and spiral spin-liquid in frustrated diamond-lattice antiferromagnets, Nat. Phys. **3**, 487 (2007).
[15] M. Brando, D. Belitz, F. M. Grosche, and T. R. Kirkpatrick, Metallic quantum ferromagnets, Rev. Mod. Phys. **88**, 025006 (2016).
[16] P. Anderson, Resonating valence bonds: A new kind of insulator? Mater. Res. Bull. **8**, 153 (1973).
[17] L. Balents, Spin liquids in frustrated magnets, Nature (London) **464**, 199 (2010).
[18] C. Broholm, R. J. Cava, S. A. Kivelson, D. G. Nocera, M. R. Norman, and T. Senthil, Quantum spin liquids, Science **367**, eaay0668 (2020).
[19] K. Binder and A. P. Young, Spin glasses: Experimental facts, theoretical concepts, and open questions, Rev. Mod. Phys. **58**, 801 (1986).
[20] S. Kundu, A. Shahee, A. Chakraborty, K. M. Ranjith, B. Koo, J. Sichelschmidt, M. T. F. Telling, P. K. Biswas, M. Baenitz, I. Dasgupta, S. Pujari, and A. V. Mahajan, Gapless quantum spin liquid in the triangular system $Sr_3CuSb_2O_9$, Phys. Rev. Lett. **125**, 267202 (2020).
[21] I. Kimchi, J. P. Sheckelton, T. M. McQueen, and P. A. Lee, Scaling and data collapse from local moments in frustrated disordered quantum spin systems, Nat. Commun. **9**, 4367 (2018).

[22] C. Dasgupta and S.-k. Ma, Low-temperature properties of the random Heisenberg antiferromagnetic chain, Phys. Rev. B **22**, 1305 (1980).

[23] M. P. Sarachik, A. Roy, M. Turner, M. Levy, D. He, L. L. Isaacs, and R. N. Bhatt, Scaling behavior of the magnetization of insulating Si:P, Phys. Rev. B **34**, 387 (1986).

[24] A. Roy, M. Sarachik, and R. Bhatt, Scaling behavior of the magnetization of Si:B, Solid State Commun. **60**, 513 (1986).

[25] R. N. Bhatt and P. A. Lee, Scaling studies of highly disordered spin-1/2 antiferromagnetic systems, Phys. Rev. Lett. **48**, 344 (1982).

[26] M. A. Paalanen, J. E. Graebner, R. N. Bhatt, and S. Sachdev, Thermodynamic behavior near a metal-insulator transition, Phys. Rev. Lett. **61**, 597 (1988).

[27] S. Bogdanovich, P. Dai, M. P. Sarachik, and V. Dobrosavljevic, Universal scaling of the magnetoconductance of metallic Si:B, Phys. Rev. Lett. **74**, 2543 (1995).

[28] A. Roy and M. P. Sarachik, Susceptibility of Si:P across the metal-insulator transition. II. Evidence for local moments in the metallic phase, Phys. Rev. B **37**, 5531 (1988).

[29] H. Murayama, T. Tominaga, T. Asaba, A. de Oliveira Silva, Y. Sato, H. Suzuki, Y. Ukai, S. Suetsugu, Y. Kasahara, R. Okuma, I. Kimchi, and Y. Matsuda, Universal scaling of specific heat in the $S = \frac{1}{2}$ quantum kagome antiferromagnet herbertsmithite, Phys. Rev. B **106**, 174406 (2022).

[30] S. Kundu, A. Hossain, P. Keerthi S., R. Das, M. Baenitz, P. J. Baker, J.-C. Orain, D. C. Joshi, R. Mathieu, P. Mahadevan, S. Pujari, S. Bhattacharjee, A. V. Mahajan, and D. D. Sarma, Signatures of a spin-$\frac{1}{2}$ cooperative paramagnet in the diluted triangular lattice of Y_2CuTiO_6, Phys. Rev. Lett. **125**, 117206 (2020).

[31] H. Murayama, Y. Sato, T. Taniguchi, R. Kurihara, X. Z. Xing, W. Huang, S. Kasahara, Y. Kasahara, I. Kimchi, M. Yoshida, Y. Iwasa, Y. Mizukami, T. Shibauchi, M. Konczykowski, and Y. Matsuda, Effect of quenched disorder on the quantum spin liquid state of the triangular-lattice antiferromagnet $1T$-TaS_2, Phys. Rev. Res. **2**, 013099 (2020).

[32] P. A. Volkov, C.-J. Won, D. I. Gorbunov, J. Kim, M. Ye, H.-S. Kim, J. H. Pixley, S.-W. Cheong, and G. Blumberg, Random singlet state in $Ba_5CuIr_3O_{12}$ single crystals, Phys. Rev. B **101**, 020406(R) (2020).

[33] K. Uematsu and H. Kawamura, Randomness-induced quantum spin liquid behavior in the $s = 1/2$ random-bond Heisenberg antiferromagnet on the pyrochlore lattice, Phys. Rev. Lett. **123**, 087201 (2019).

[34] See Supplemental Material at http://link.aps.org/supplemental/10.1103/PhysRevB.110.L020406 for further details about sample preparation, experimental conditions, x-ray diffraction, the magnetic susceptibility analysis, estimation of lattice heat capacity, and analytical theoretical calculations, which includes Refs. [35,38–42].

[35] M.-E. Song, D. Maurya, Y. Wang, J. Wang, M.-G. Kang, D. Walker, P. A. Thomas, S. T. Huxtable, R. J. Bodnar, N. Q. Vinh, and S. Priya, Phase transitions and phonon mode dynamics of $Ba(Cu_{1/3}Nb_{2/3})O_3$ and $Sr(Cu_{1/3}Nb_{2/3})O_3$ for understanding thermoelectric response, ACS Appl. Energy Mater. **3**, 3939 (2020).

[36] Y. Singh, Y. Tokiwa, J. Dong, and P. Gegenwart, Spin liquid close to a quantum critical point in $Na_4Ir_3O_8$, Phys. Rev. B **88**, 220413(R) (2013).

[37] T. Dey, M. Majumder, J. C. Orain, A. Senyshyn, M. Prinz-Zwick, S. Bachus, Y. Tokiwa, F. Bert, P. Khuntia, N. Büttgen, A. A. Tsirlin, and P. Gegenwart, Persistent low-temperature spin dynamics in the mixed-valence iridate $Ba_3InIr_2O_9$, Phys. Rev. B **96**, 174411 (2017).

[38] H. D. Zhou, E. S. Choi, G. Li, L. Balicas, C. R. Wiebe, Y. Qiu, J. R. D. Copley, and J. S. Gardner, Spin liquid state in the $S = 1/2$ triangular lattice $Ba_3CuSb_2O_9$, Phys. Rev. Lett. **106**, 147204 (2011).

[39] T. Dey, A. V. Mahajan, P. Khuntia, M. Baenitz, B. Koteswararao, and F. C. Chou, Spin-liquid behavior in $J_{\text{eff}} = \frac{1}{2}$ triangular lattice compound $Ba_3IrTi_2O_9$, Phys. Rev. B **86**, 140405(R) (2012).

[40] C. Y. Jiang, Y. X. Yang, Y. X. Gao, Z. T. Wan, Z. H. Zhu, T. Shiroka, C. S. Chen, Q. Wu, X. Li, J. C. Jiao, K. W. Chen, Y. Bao, Z. M. Tian, and L. Shu, Spin excitations in the quantum dipolar magnet $Yb(BaBO_3)_3$, Phys. Rev. B **106**, 014409 (2022).

[41] K. Somesh, S. S. Islam, S. Mohanty, G. Simutis, Z. Guguchia, C. Wang, J. Sichelschmidt, M. Baenitz, and R. Nath, Absence of magnetic order and emergence of unconventional fluctuations in the $J_{\text{eff}} = \frac{1}{2}$ triangular-lattice antiferromagnet $YbBO_3$, Phys. Rev. B **107**, 064421 (2023).

[42] S. Mohanty, S. S. Islam, N. Winterhalter-Stocker, A. Jesche, G. Simutis, C. Wang, Z. Guguchia, J. Sichelschmidt, M. Baenitz, A. A. Tsirlin, P. Gegenwart, and R. Nath, Disordered ground state in the spin-orbit coupled $J_{\text{eff}} = \frac{1}{2}$ distorted honeycomb magnet $BiYbGeO_5$, Phys. Rev. B **108**, 134408 (2023).